Journal of Electroanalytical Chemistry 765 (2016) 100–104

Contents lists available at ScienceDirect

Journal of Electroanalytical Chemistry

journal homepage: www.elsevier.com/locate/jelechem

Effect of ligand protonation on the facilitated ion transfer reactions across oil|water interfaces. V. Applications of forced hydrodynamic conditions

Franco Vega Mercado, Juan Manuel Ovejero, Ricardo Ariel Fernández, Sergio Alberto Dassie *

Instituto de Investigaciones en Fisicoquímica de Córdoba (INFIQC), CONICET, Departamento de Fisicoquímica, Facultad de Ciencias Químicas, Universidad Nacional de Córdoba, X5000HUA, Ciudad Universitaria, Córdoba, Argentina

ARTICLE INFO

Article history:
Received 15 May 2015
Received in revised form 30 July 2015
Accepted 2 August 2015
Available online 5 August 2015

Keywords:
Facilitated proton transfer
Forced hydrodynamic conditions
Liquid|liquid interface
Water autoprotolysis
Quinidine

ABSTRACT

Hydrodynamic forced conditions applied to the aqueous or the organic phase during a potential sweep can be used to elucidate the mechanisms of ion transfer across liquid|liquid interfaces. The aim of this study is to confirm experimentally the previous proposed global mechanisms of facilitated proton transfer via water autoprotolysis and to extend them, controlling the mass transport. We show that proton transfer assisted by quinidine via water autoprotolysis is an interesting example, where the ion transfer reaction occurs with the formation of different products in each phase, i.e., protonated weak base in the organic phase and the hydroxide ion in the aqueous phase. Furthermore, one of the reactants (water) is always in excess with respect to the other one (neutral weak base). These features provide unique characteristics to facilitated proton transfer via water autoprotolysis to be explored by applying forced hydrodynamic conditions.

© 2015 Elsevier B.V. All rights reserved.

1. Introduction

The transfer of protonated species across liquid|liquid interfaces is reported in several experimental works in the literature. In many of these studies, the transfer of weak acids and bases has been found to depend on the pH of the aqueous phase and on their partition coefficient [1–35]. A theoretical approach for modeling the facilitated proton transfer or protonatable species transfer was developed by Girault and coworkers [12] and Sawada and Osakai [16]. In a previous series of papers [25,29,36,37], we have derived the general equations for a model of ion transfer reactions across the oil|water interface assisted by a neutral weak base. Those analyses were focused on studying the effect of water autoprotolysis on the transfer processes by comparing implicitly or explicitly buffered solution with unbuffered solution models. In some conditions, as in strongly buffered solutions, it must be taken into account that the autoprotolysis reaction may not be relevant, but in other cases, the omission of this reaction might affect the shape of voltammograms, and, relevantly, some transfer reaction may not even occur [36]. In a second approach of this model [25], we solved the equations for the protonatable species transfer using explicit finite difference. This method allows obtaining information of the diffusion layer. In addition, it is possible to assign different diffusion coefficients for each species involved in the transfer mechanism. The model was corroborated by experimental results obtained from the quinine transfer across the H_2O|1,2-dichloroethane interface, and the involved ion transfer mechanism was analyzed in terms of the current-potential and theoretical concentration profiles [25]. Finally, we have presented an extension of our last model in which a buffered solution with multiple acid–base equilibria was explicitly considered [29]. The observed results show the importance of the water autoprotolysis reaction in this model. In the other hand, this model was solved using explicit finite difference with exponentially expanding space grid [38]. The reported equations allow simulating the system under different conditions. We have analyzed pH changes and buffer capacity at the interface and in the diffusion layer during the potential scan sweep. This model was also corroborated with the experimental results found for the quinine transfer across the H_2O|1,2-dichloroethane interface in the presence of phosphate buffer for different buffer capacities of the aqueous phase [29]. Recently, we developed the equations for the half-wave potential of facilitated proton transfer or protonated species transfer across liquid|liquid interfaces, including ion pairing. The main equation that was developed in this research allows simulating different chemical systems (hydrophilic and hydrophobic neutral bases, multiple protonated species, ion-pair formation in the organic phase) [39].

The electrochemical study of ion transfer at the interface between two immiscible electrolyte solutions (ITIES) has allowed the determination of relevant thermodynamic and transport parameters, provided the ion transfer processes measured are limited by mass diffusion. For the study of kinetic parameters and mechanistic information, the mass transfer rate must be increased. Different experimental approaches have been employed in order to obtain a high mass-transport rate [40–54]. In particular, imposition of a convective flow to increase the mass-transport has also been reported [47–54]. An alternative approach

* Corresponding author.
E-mail address: sdassie@fcq.unc.edu.ar (S.A. Dassie).

http://dx.doi.org/10.1016/j.jelechem.2015.08.001
1572-6657/© 2015 Elsevier B.V. All rights reserved.

to the study of liquid|liquid extraction processes involves the rotating diffusion cell (RDC), introduced by Albery and co-workers [55–57] and modified by Manzanares et al. [58] and Kralj and Dryfe [59] in order to study the simple and facilitated ion transfer reactions by external polarization. Fujii et al. [60] performed measurements of ion transfer reaction at a rotating liquid membrane disk electrode (LMDE) and a rotating liquid membrane ring–liquid membrane disk electrode (LMRE–LMDE).

Hydrodynamic voltammetry was also reported at ITIES, using an RDC configuration. The voltammetry arises from laminar flow, induced separately in the organic and aqueous phases of the ITIES. The ITIES have been stabilized by a polyester track-etched membrane material. This methodology has been used to determine reaction mechanisms and kinetic parameters for reactions involving liquid|liquid interfaces [59]. Then, this alternative procedure was extended to the study of facilitated ion transfer across the water|1,2-dichloroethane interface [61]. Recently, Dryfe et al. [62] presented a novel method, which employed an organic membrane fitted on the liquid|liquid interface and therefore, it allowed rotation of the interface, for the determination of the diffusion coefficient of weakly ionized species. The limiting current as a function of rotating rate was measured in this RDC based configuration [63] and the Levich equation was used to determine the diffusion coefficient values.

On the other hand, Wilke et al. [64] have proposed an alternative methodology consisting in alternately stirring the aqueous or organic phase during the potential sweep to elucidate ion transfer mechanisms across ITIES. In this experimental setup, the convective flux in one phase produced an asymmetry of the diffusion field, that is, a selective decrease in the thickness of the diffusion layer on one side of the interface. This allows distinguishing the direction of the ion transfer. This methodology has been used to elucidate the mechanism of the electrochemical transfer of different ionized species [28,64–66]. Recently, we presented the general equations for a model that describes ion transfer reactions across the oil|water interface assisted by a neutral ligand, under forced hydrodynamic conditions. Analysis was mainly focused on the effect of mechanical stirring of the aqueous or organic phase during the potential sweep, and its influence on the limiting diffusion currents [67].

In this paper, we present an experimental analysis of the effect of forced hydrodynamic conditions applied to each phase of the system on the current-potential profiles. This analysis is focused on proton transfer assisted by quinidine via water autoprotolysis. The aim of these studies is to confirm experimentally previous proposed global mechanisms [25,29,36,37] and to extend them with a controlled mass transport.

2. Experimental

The electrochemical experiments were performed in a four-electrode system using a conventional glass cell of interfacial area 0.18 cm^2. Two platinum wires were used as counter-electrodes and the reference electrodes were Ag|AgCl|Cl^-. The reference electrode in contact with the organic solution was immersed in an aqueous solution of 1.0×10^{-2} M tetrapentylammonium bromide (TPnABr) (Aldrich) and 1.0×10^{-2} M LiCl (J.T. Baker, p.a.).

The potential values (E) reported are the applied potentials, which include $\Delta_o^w\phi^{o'}_{tr,TPnA^+} = -0.361$ V for the transfer of the reference ion $TPnA^+$ [68]. The base electrolyte is LiCl (J.T. Baker, p.a.) 1.0×10^{-2} M in ultrapure water and 1.0×10^{-2} M tetrapentylammonium tetrakis (4-chlorophenyl) borate (TPnATCl-PB) in 1,2-dichloroethane (1,2-DCE) (Dorwil, p.a.). TPnATCl-PB was prepared as described in [69]. Quinidine hydrochloride monohydrate (Sigma) was dissolved in the aqueous phase and the pH values were adjusted using concentrated LiHO (Anedra, p.a.). All reagents and solvents were used as received.

Quinidine is an organic anti-arrhythmic drug whose neutral species (B) is poorly soluble in aqueous solutions but it can form soluble singly protonated (HB^+) or doubly protonated (H_2B^{2+}) species in acidic aqueous solution [10,11]. The acid–base equilibrium constants of quinidine in aqueous solutions are $pK^w_{a,1} = 4.43 \pm 0.02$ and $pK^w_{a,2} = 8.66 \pm 0.02$ whereas their values in the organic phase are $pK^o_{a,1} = 9.7 \pm 0.2$ and $pK^o_{a,2} = 14.2 \pm 0.2$ [10,11]. The formal potential transfer values of singly-charged quinidine and doubly-charged quinidine at the H_2O|1,2-DCE interface are equal to $\Delta_o^w\phi^{0'}_{HB^+} = 0.080 \pm 0.009$ V and $\Delta_o^w\phi^{0'}_{H_2B^{2+}} = 0.162 \pm 0.04$ V, respectively [10,11]. Finally, the partition coefficient of the neutral form of the quinidine at the H_2O|1,2-DCE interface is equal to 2.50 ± 0.04 [10,11].

Cyclic voltammetry was performed using a potentiostat which eliminates the *IR* drop automatically by means of a periodic current-interruption technique [70]. A Hi-Tek Instruments waveform generator and a data acquisition system were also employed.

Forced hydrodynamic conditions (FHCs) were performed with a polytetrafluoroethylene (PTFE) cylinder analogue to a rotating-disk electrode, controlled by a PINE disk rotator [64]. The experimental procedure consists to apply FHCs in one phase, while the other phase is in quiescent conditions [64]. All the current-potential profiles are presented as raw data (without mathematical post-processing).

All the voltammograms shown in this work were measured with solutions in acid–base and partition equilibria [25,26,28,29,66]. Different amounts of aqueous and organic phases were stirred until equilibrium between them was reached (initial system). This was performed in a stoppered flask for 1 h. The volume ratio (r) is defined as the ratio between the organic phase (V_o) and the aqueous phase (V_w) volumes. We used for all the electrochemical experiments $r = 0.30$ (V_o = 6.0 mL and $V_w = 20$ mL). After equilibration, the electrochemical cell was filled with an aliquot of 6 mL of the aqueous phase and 4 mL of the organic phase. The aliquots were taken from the bulk of each phase in contact, to assure that their intensive properties (i.e., species concentrations) were the equilibrium properties. Thus, the electrochemical cell was composed by two equilibrated solutions with the same properties as those of the initial system.

3. Results and discussion

The experimental system selected in this work is based on a hydrophobic weak base (quinidine), which presents different global charge (ion) transfer mechanisms. These mechanisms depend of the initial pH value or the initial species in each phase [25,29]. The chemical reactions in each phase as well as the heterogeneous ion transfer reactions involved in this system were already described [25,29,36,37]. These mechanisms are summarized in Scheme 1 for simple protonated species transfer reaction (panel (a)) and facilitated proton transfer reactions by a neutral weak base (B) present in the organic phase (panels (b) and (c)). In particular, a facilitated proton transfer via water autoprotolysis is schematized in panel (c).

The transfer behavior of quinidine was investigated by cyclic voltammetry at the water|1,2-DCE interface and is shown in this section. Fig. 1 shows the current-potential profiles obtained at two different initial pH values in quiescent conditions. At pH 6.5, two well defined ion transfer processes were observed. The first process (PI) occurs at ca. 0.50 V and the second one (PII) at ca. 0.75 V. PI is associated with singly protonated species transfer or facilitated proton transfer according to the following global ion transfer mechanisms [25,29,36,37]:

$$HB^+(w) \rightleftharpoons HB^+(o) \qquad R(I)$$

or

$$H^+(w) + B(o) \rightleftharpoons HB^+(o) \qquad R(II)$$

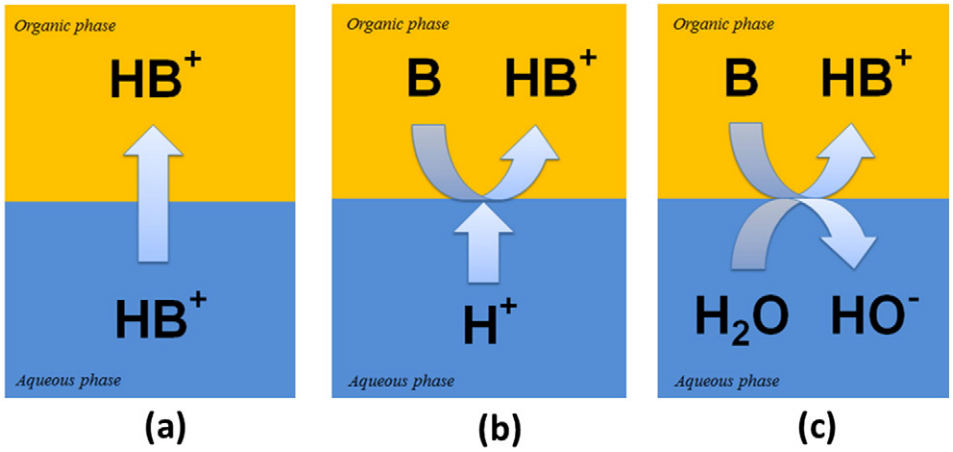

Scheme 1. Schematic global mechanisms of assisted proton transfer for forward potential sweep. Simple protonated species transfer (a), facilitated proton transfer (b), and facilitated proton transfer via water autoprotolysis (c).

while PII corresponds to facilitated proton transfer via water autoprotolysis [25,29,36,37]:

$$H_2O + B(o) \rightleftharpoons HB^+(o) + HO^-(w). \qquad R(III)$$

The potential difference of 0.25 V between the first and second processes (PI and PII) measured at pH 6.5, is related to the extra energy required to breakdown water molecules to produce the protons involved in the transfer of the singly-protonated species to the organic phase [71]. At pH 9.7, a unique ion transfer process was observed for the forward potential sweep, which corresponds to PII (R(III)). On the other hand, two different ion transfer processes were observed in the backward potential sweep. The electrochemical process at ca. 0.70 V corresponds to PII, and the second current peak (0.45 V) is related to the transfer of protonated species remained in the organic phase [25]. This behavior is due to the high HO^- mobility that diffuses into the bulk of the aqueous phase, which is responsible of a depletion of the interfacial amount of this ion. Then, the HO^- concentration at the interface is lower than the expected concentration and the backward reaction corresponding to (PII) occurs to a lower extent. Facilitated proton transfer via water autoprotolysis is an interesting example where the ion transfer reaction occurs with the formation of different products in each phase, i.e., protonated weak base in the organic phase and the hydroxide ion in the aqueous phase (see Scheme 1, panel (c)). Furthermore, one of the reactants (water) is always in excess with respect to the other one (neutral weak base). These features provide unique characteristics to facilitate proton transfer via water autoprotolysis to be explored by applying FHCs.

According to the used experimental procedure, FHCs were applied by stirring one phase while the other one remained in quiescent conditions. Therefore, the species in the stirred solution behave under diffusion-convective regime while only diffusion transport takes place in the other phase [64]. When FHCs are applied, the species are uniformly distributed into the bulk solution and diffusional transport is modified by controlling the diffusion-layer thickness [72]. At higher stirring frequencies, the diffusion layers are thinner in the stirred phase, thus larger concentration gradients are produced causing observable changes on the current-potential profiles. Fig. 2 shows the voltammograms measured at pH 6.5 under FHCs applied to the organic phase. As it can be observed, PI is not affected during the forward potential sweep, but progressively diminishes during the backward potential sweep. This result strongly indicates that the ion transfer process is controlled by the diffusion of the species in the quiescent aqueous phase. In consequence, PI corresponds mainly to a simple transfer mechanism of protonated weak base initially present in the aqueous phase as shown in Scheme 1 (R(I)). In contrast, the shape of the electrochemical wave and the current values of the second process, at ca. 0.75 V, are clearly modified. The absence of negative current values in the backward potential sweep measured at high stirring frequencies indicates that the

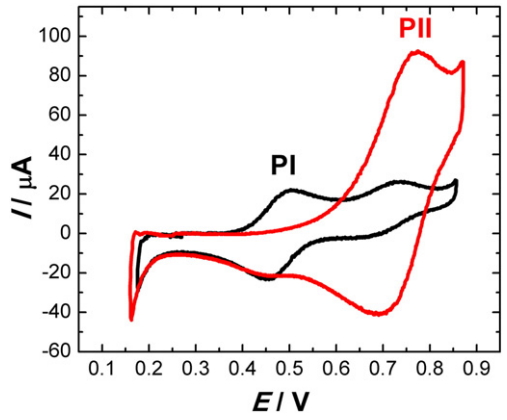

Fig. 1. Cyclic voltammograms for the transfer of quinidine at two different pH values. Quiescent solutions at pH 6.5 (—) and 9.7 (—). Organic phase: TPnATCl-PB 1×10^{-2} M. Aqueous phase: LiCl 1×10^{-2} M + 1×10^{-3} M of quinidine. r = 0.30; v = 0.050 V s^{-1}.

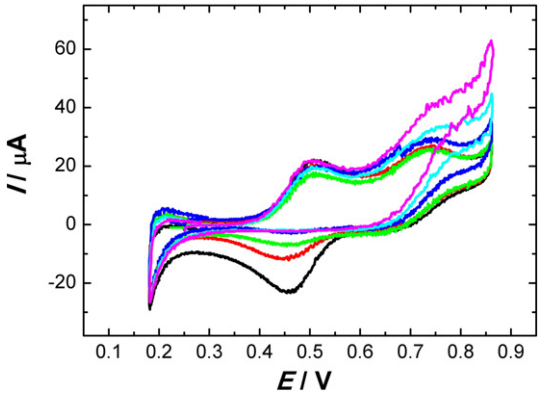

Fig. 2. Cyclic voltammograms for the transfer of quinidine at pH 6.5. Quiescent solution (—). Organic phase stirred at 300 rpm (—), 500 rpm (—), 700 rpm (—), 1400 rpm (—), and 2200 rpm (—). Organic phase: TPnATCl-PB 1×10^{-2} M. Aqueous phase: LiCl 1×10^{-2} M + 1×10^{-3} M of quinidine. r = 0.30; v = 0.050 V s^{-1}.

net cation flux is mainly from the aqueous to the organic phase. Hence, PII corresponds to a facilitated proton transfer process (R(III)). Moreover, noting that this process takes place at a higher potential than PI, this ion transfer process requires an extra energy in agreement with the proton facilitated transfer via water autoprotolysis reaction (Scheme 1, panel (c) and R(III)) [36]. When water autoprotolysis reaction occurs, the electrochemically generated HO^- ions diffuse from the interface into the bulk of the aqueous phase, and these neutralize the protonated weak base.

Successive potential sweeps provide great information about the global ion transfer mechanism. In particular, in the second potential sweep, the current depends on the electrogenerated species at the interface in the previous sweep. Fig. 3a) compares the first and second voltammograms of the system described in Fig. 2. As expected, the current peak of PI decreases at the forward second cycle, because the protonated weak base was consumed by the neutralization reaction with the electrochemically generated HO^- ions in the aqueous phase. On the other hand, the shape of the current-potential profile and the current value of PII are not changed during the cycling because the diffusion-layer thickness in the organic phase remains constant. It is important to note that, the shape and the current values of the voltammograms obtained in quiescent solutions are not changed during the cycling (data not shown). Moreover, second cycles measured at different stirring frequencies indicate that PI current peaks decrease when increasing the stirring frequencies, because the neutralization reaction spreads over longer distance from the aqueous side of the interface

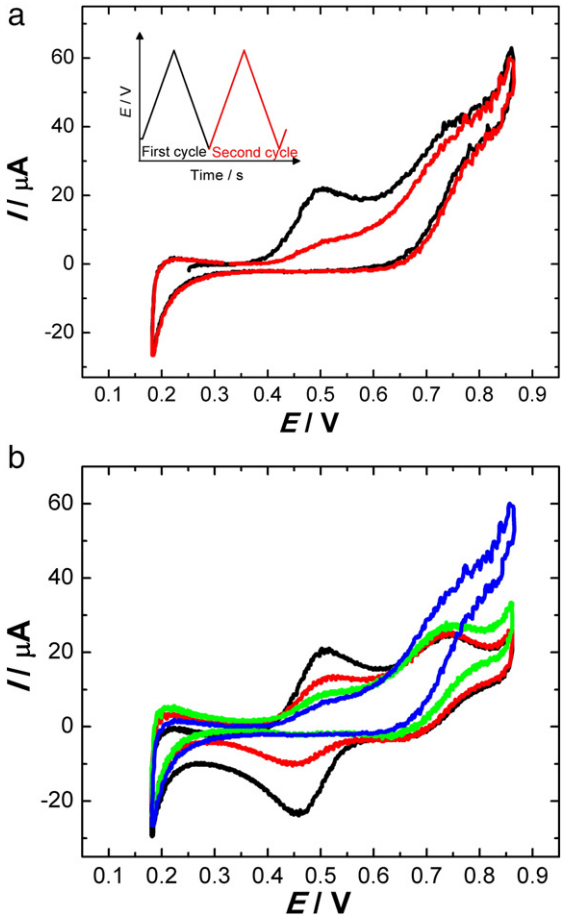

Fig. 3. Cyclic voltammograms for the transfer of quinidine at pH 6.5. a) First (—) and second cycle (—) experiments. Organic phase stirred at 2200 rpm. b) Second cycles of quiescent solutions (—) and organic phase stirred at 300 rpm (—); 700 rpm (—); 2200 rpm (—). Organic phase: TPnATCl-PB 1×10^{-2} M. Aqueous phase: LiCl 1×10^{-2} M + 1×10^{-3} M of quinidine. r = 0.30; v = 0.050 V s^{-1}.

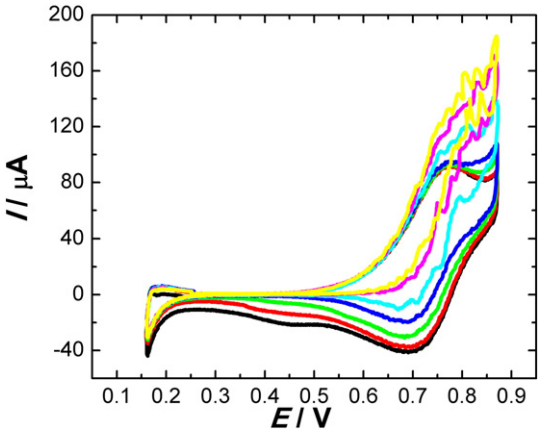

Fig. 4. Cyclic voltammograms for the transfer of quinidine at pH 9.7. Quiescent solution (—). Organic phase stirred at 500 rpm (—), 700 rpm (—), 900 rpm (—), 1200 rpm (—), 1600 rpm (—), and 2000 rpm (—). r = 0.30; v = 0.050 V s^{-1}.

(Fig. 3b)). At higher stirring frequencies, the diffusion-layer thickness decreases; thus, a larger amount of singly-charged quinidine is transferred together with a stronger HO^- production at the interface. These HO^- ions diffuse from the interface to the bulk of the aqueous phase (quiescent solution) and neutralize the HB^+ species which are moving from the bulk of the phase to the interface. Moreover, this behavior was also observed for the third cycle (data not shown).

Fig. 4 depicts the effect to apply FHCs to the organic phase at pH 9.7. In this case, a unique ion transfer process can be observed for the forward potential sweep that corresponds to PII, because the HB^+ concentration in the aqueous phase is negligible. As explained above, the application of FHCs decreases the diffusion-layer thickness and the protonated species are uniformly distributed in the organic phase. In consequence, an increment in the current values in the forward potential sweep is observed when the stirring frequencies are increased. Thus, the interfacial pH increases. In the backward potential sweep, the second current peak (0.45 V) decreases, because the singly protonated species that remained in the organic phase are uniformly distributed.

Fig. 5 shows cyclic voltammograms measured at pH 9.7 with FHCs applied to the aqueous phase. The profiles slightly change in the forward potential sweep. On the contrary, the backward potential sweep shows an important diminution in the current values of PII when the stirring frequencies increase, with the concomitant appearance of a new ion transfer process at ca. 0.45 V. Under these applied FHCs, the HO^- ions are uniformly distributed in the aqueous phase. Therefore,

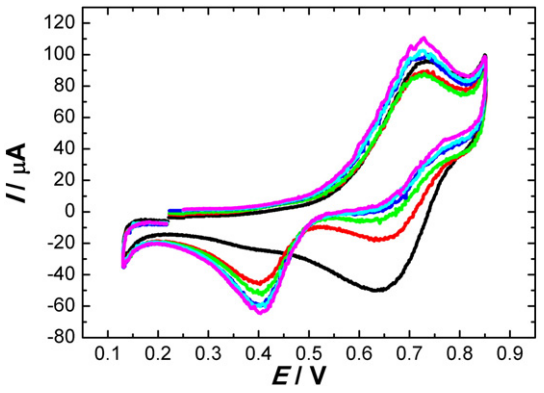

Fig. 5. Cyclic voltammograms for the transfer of quinidine at pH 9.7. Quiescent solution (—). Aqueous phase stirred at 300 rpm (—); 500 rpm (—); 900 rpm (—); 1200 rpm (—); and 1600 rpm (—). Organic phase: TPnATCl-PB 1×10^{-2} M. Aqueous phase: LiCl 1×10^{-2} M + 1×10^{-3} M of quinidine. r = 0.30; v = 0.050 V s^{-1}.

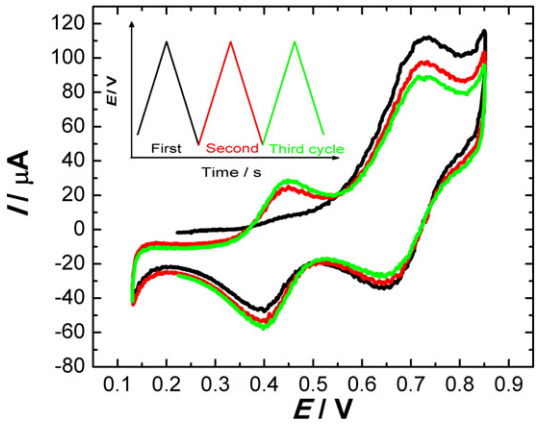

Fig. 6. First (—), second (—) and third (—) potential sweeps of cyclic voltammograms for the transfer of quinidine at pH 9.7. Aqueous phase stirred at 300 rpm. Organic phase: TPnATCl-PB 1×10^{-2} M. Aqueous phase: LiCl 1×10^{-2} M + 1×10^{-3} M of quinidine. r = 0.30; v = 0.075 V s^{-1}.

the backward reaction of PII cannot occur without HO^- ions at the interface. This change in the backward ion transfer reaction occurs because HB^+ is stable in the organic phase at this potential range (PII). Fig. 6 compares three potential cycles measured with FHCs applied to aqueous phase. The current peaks of PI increase in the forward potential sweep of the successive cycles, because HB^+, in the aqueous side of the interface, can be transferred in this potential range. Moreover, the current peaks of PII decrease in the forward potential sweep of the successive cycles.

4. Conclusions

Global proton transfer mechanisms at liquid|liquid interface can be easily evaluated by cyclic voltammetry combined with forced hydrodynamic conditions applied to each phase. Besides, the ion transfer mechanism can be modified by controlling the mass transport in each phase. This simple experimental procedure allows confirming the proposed proton transfer mechanism via water autoprotolysis (R(III)). The HO^- ions electrochemically generated at the interface can be used as a reactant in several coupled chemical reactions like nanoparticle synthesis and nucleophilic substitutions. These chemical reactions can be externally tuned by the applied potential and the forced hydrodynamic conditions in each or both phases opening a wide range of possibilities in new synthetic routes.

Acknowledgments

R.A.F. and S.A.D. are Researchers from Consejo Nacional de Investigaciones Científicas y Tecnológicas (CONICET). J.M.O. and F.V.M. thank CONICET for the fellowships granted. Financial support from CONICET and Secretaría de Ciencia y Tecnología (SECyT-UNC) and ANPCyT PICT 2012-1820 are gratefully acknowledged.

References

[1] Z. Yoshida, H. Freiser, J. Electroanal. Chem. 162 (1984) 307.
[2] D. Homolka, V. Mareček, Z. Samec, K. Baše, H. Wendt, J. Electroanal. Chem. 163 (1984) 159.
[3] Y. Liu, E. Wang, J. Chem. Soc. Faraday Trans. I 83 (1987) 2993.
[4] H. Doe, K. Yoshioka, T. Kitagawa, J. Electroanal. Chem. 324 (1992) 69.
[5] L.M. Yudi, A.M. Baruzzi, J. Electroanal. Chem. 328 (1992) 153.
[6] K. Kontturi, L. Murtomäki, J. Pharm. Sci. 81 (1992) 970.
[7] L.M. Yudi, A.M. Baruzzi, V.M. Solis, J. Electroanal. Chem. 360 (1993) 211.
[8] S.A. Dassie, L.M. Yudi, A.M. Baruzzi, Electrochim. Acta 40 (1995) 2953.
[9] F. Reymond, G. Steyaert, A. Pagliara, P. Carrupt, B. Testa, H.H. Girault, Helv. Chim. Acta 79 (1996) 1651.
[10] F. Reymond, G. Steyaert, P.-A. Carrupt, B. Testa, H.H. Girault, J. Am. Chem. Soc. 118 (1996) 11951.
[11] F. Reymond, G. Steyaert, P.-A. Carrupt, B. Testa, H.H. Girault, Helv. Chim. Acta 79 (1996) 101.
[12] F. Reymond, P.-F. Brevet, P.-A. Carrupt, H.H. Girault, J. Electroanal. Chem. 424 (1997) 121.
[13] Z. Ding, F. Reymond, P. Baumgartner, D.J. Fermín, P.-F. Brevet, P. Carrupt, H.H. Girault, Electrochim. Acta 44 (1998) 3.
[14] Y. Kubota, H. Katano, K. Maeda, M. Senda, Electrochim. Acta 44 (1998) 109.
[15] Z. Samec, J. Langmaier, A. Trojánek, E. Samcová, J. Málek, Anal. Sci. 14 (1998) 35.
[16] S. Sawada, T. Osakai, Phys. Chem. Chem. Phys. 1 (1999) 4819.
[17] F. Reymond, P.-A. Carrupt, B. Testa, H.H. Girault, Chem. Eur. J. 5 (1999) 39.
[18] A.I. Azcurra, L.M. Yudi, A.M. Baruzzi, J. Electroanal. Chem. 461 (1999) 194.
[19] F. Reymond, V. Chopineaux-Courtois, G. Steyaert, G. Bouchard, P.-A. Carrupt, B. Testa, H.H. Girault, J. Electroanal. Chem. 462 (1999) 235.
[20] W. Wickler, A. Mönner, E. Uhlemann, S. Wilke, H. Müller, J. Electroanal. Chem. 469 (1999) 91.
[21] M. Senda, Y. Kubota, H. Katano, Liq. Interfaces Chem. Biol. Pharm. Appl. 2001, pp. 683–698.
[22] Y. Kubota, H. Katano, M. Senda, Anal. Sci. 17 (2001) 65.
[23] H. Alemu, Pure Appl. Chem. 76 (2004) 697.
[24] R.A. Fernández, S.A. Dassie, J. Electroanal. Chem. 585 (2005) 240.
[25] J.I. Garcia, R.A. Iglesias, S.A. Dassie, J. Electroanal. Chem. 586 (2006) 225.
[26] J.I. Garcia, R.A. Fernández, A.J. Ruggeri, S.A. Dassie, J. Electroanal. Chem. 594 (2006) 80.
[27] M. Rimboud, C. Elleouet, F. Quentel, J.-M. Kerbaol, M. L'Her, J. Electroanal. Chem. 622 (2008) 233.
[28] R.A. Fernández, M.I. Velasco, L.I. Rossi, S.A. Dassie, J. Electroanal. Chem. 650 (2010) 47.
[29] J.I. Garcia, M.B. Oviedo, S.A. Dassie, J. Electroanal. Chem. 645 (2010) 1.
[30] A. Trojánek, J. Langmaier, S. Záliš, Z. Samec, Electrochim. Acta 110 (2013) 816.
[31] E. Torralba, J.A. Ortuño, A. Molina, C. Serna, F. Karimian, Anal. Chim. Acta 826 (2014) 12.
[32] B. Li, Y. Qiao, J. Gu, X. Zhu, X. Yin, Q. Li, Z. Zhu, M. Li, P. Jing, Y. Shao, J. Electroanal. Chem. 726 (2014) 21.
[33] M. Velicky, A.N.J. Rodgers, R.A.W. Dryfe, K.Y. Tam, ADMET DMPK 2 (2014) 143.
[34] Z. Mandic, ADMET DMPK 2 (2014) 168.
[35] M. Sairi, D.W.M. Arrigan, Talanta 132 (2015) 205.
[36] S.A. Dassie, J. Electroanal. Chem. 578 (2005) 159.
[37] S.A. Dassie, J. Electroanal. Chem. 585 (2005) 256.
[38] D. Britz, Digital Simulation in Electrochemistry, 3rd ed. Springer, Berlin Heidelberg, 2005.
[39] S.A. Dassie, J. Electroanal. Chem. 728 (2014) 51.
[40] Z. Samec, Pure Appl. Chem. 76 (2004) 2147.
[41] R.A. Iglesias, S.A. Dassie, Ion Transfer at Liquid/Liquid Interfaces, Nova Publishers, New York, 2010.
[42] G. Taylor, H.H. Girault, J. Electroanal. Chem. 208 (1986) 179.
[43] Y. Ohkouchi, T. Kakutani, T. Osakai, M. Senda, Anal. Sci. 7 (1991) 371.
[44] J.A. Campbell, H.H. Girault, J. Electroanal. Chem. 266 (1989) 465.
[45] A.A. Stewart, G. Taylor, H.H. Girault, J. McAleer, J. Electroanal. Chem. 296 (1990) 491.
[46] A.A. Stewart, Y. Shao, C.M. Pereira, H.H. Girault, J. Electroanal. Chem. 305 (1991) 135.
[47] J. Koryta, P. Vanýsek, M. Březina, J. Electroanal. Chem. 67 (1976) 263.
[48] S. Kihara, M. Suzuki, K. Maeda, K. Ogura, M. Matsui, J. Electroanal. Chem. 210 (1986) 147.
[49] S. Wilke, H. Franzke, H. Müller, Anal. Chim. Acta 268 (1992) 285.
[50] S. Wilke, Anal. Chim. Acta 295 (1994) 165.
[51] B. Hundhammer, T. Solomon, T. Zerihun, M. Abegaz, A. Bekele, K. Graichen, J. Electroanal. Chem. 371 (1994) 1.
[52] V. Mareček, H. Jänchenová, M.P. Colombini, P. Papoff, J. Electroanal. Chem. 217 (1987) 213.
[53] P. Liljeroth, C. Johans, K. Kontturi, J.A. Manzanares, J. Electroanal. Chem. 483 (2000) 37.
[54] S.S. Hill, R.A.W. Dryfe, E.P.L. Roberts, A.C. Fisher, K. Yunus, Anal. Chem. 75 (2003) 486.
[55] W.J. Albery, A.M. Couper, J. Hadgraft, C. Ryan, J. Chem. Soc. Faraday Trans. 70 (1974) 1124.
[56] J. Albery, J.F. Burke, E.B. Leffler, J. Hadgraft, J. Chem. Soc. Faraday Trans. 72 (1976) 1618.
[57] W.J. Albery, R.A. Choudhery, J. Phys. Chem. 92 (1988) 1142.
[58] J.A. Manzanares, R. Lahtinen, B. Quinn, K. Kontturi, D.J. Schiffrin, Electrochim. Acta 44 (1998) 59.
[59] B. Kralj, R.A.W. Dryfe, J. Phys. Chem. B 106 (2002) 6732.
[60] K. Fujii, S. Tanibuchi, S. Kihara, Anal. Sci. 21 (2005) 1415.
[61] B. Kralj, R.A.W. Dryfe, J. Electroanal. Chem. 560 (2003) 127.
[62] M. Velický, K.Y. Tam, R.A.W. Dryfe, J. Electroanal. Chem. 683 (2012) 94.
[63] M. Velický, K.Y. Tam, R.A.W. Dryfe, Anal. Chem. 84 (2012) 2541.
[64] N. Wilke, R.A. Iglesias, S.G. Chesniuk, S.A. Dassie, A.M. Baruzzi, Bull. Chem. Soc. Jpn. 75 (2002) 235.
[65] M.A. Fernández, L.M. Yudi, A.M. Baruzzi, Electroanalysis 16 (2004) 491.
[66] R.A. Fernández, S.A. Dassie, J. Electroanal. Chem. 624 (2008) 121.
[67] J.M. Ovejero, R.A. Fernández, S.A. Dassie, J. Electroanal. Chem. 666 (2012) 42.
[68] J. Czapkiewicz, B. Czapkiewicz-Tutaj, J. Chem. Soc. Faraday Trans. I 76 (1980) 1663.
[69] H. Katano, M. Senda, Anal. Sci. 12 (1996) 683.
[70] A.M. Baruzzi, J. Ühlken, J. Electroanal. Chem. 282 (1990) 267.
[71] S.A. Dassie, J. Electroanal. Chem. 643 (2010) 20.
[72] V.S. Bagotsky, Fundamentals of Electrochemistry, John Wiley & Sons, New Jersey, 2008.